The Astrophysical Journal, 817:151 (7pp), 2016 February 1 doi:10.3847/0004-637X/817/2/151

RAPID DECREASING IN THE ORBITAL PERIOD OF THE DETACHED WHITE DWARF–MAIN SEQUENCE BINARY SDSS J143547.87+373338.5

S.-B. Qian[1,2,3], Z.-T. Han[1,2,3], B. Soonthornthum[4], L.-Y. Zhu[1,2,3], J.-J. He[1,2], S. Rattanasoon[4], S. Aukkaravittayapun[4], W.-P. Liao[1,2], E.-G. Zhao[1,2,3], J. Zhang[1,2], and E. Fernández Lajús[5,6,7]

[1] Yunnan Observatories, Chinese Academy of Sciences (CAS), P.O. Box 110, 650011 Kunming, P. R. China; qsb@ynao.ac.cn
[2] Key Laboratory of the Structure and Evolution Celestial Bodies, Chinese Academy of Sciences, P.O. Box 110, 650011 Kunming, P. R. China
[3] University of the Chinese Academy of Sciences, Yuquan Road 19#, Sijingshang Block, 100049 Beijing, P. R. China
[4] National Astronomical Research Institute of Thailand, 191 Siriphanich Bldg., Huay Kaew Rd., Chiang Mai 50200, Thailand
[5] Facultad de Ciencias Astronómicas y Geofiísicas, Universidad Nacional de La Plata, 1900 La Plata, Buenos Aires, Argentina
[6] Instituto de Astrofisica de La Plata (CCT La plata—CONICET/UNLP), Argentina

Received 2015 June 23; accepted 2015 December 9; published 2016 January 28

ABSTRACT

SDSS J143547.87+373338.5 is a detached eclipsing binary that contains a white dwarf with a mass of 0.5 $M_{\odot}$ and a fully convective star with a mass of 0.21 $M_{\odot}$. The eclipsing binary was monitored photometrically from 2009 March 24 to 2015 April 10, by using two 2.4-m telescopes in China and in Thailand. The changes in the orbital period are analyzed based on eight newly determined eclipse times together with those compiled from the literature. It is found that the observed–calculated (O–C) diagram shows a downward parabolic change that reveals a continuous period decrease at a rate of $\dot{P} = -8.04 \times 10^{-11}$ s s^{-1}. According to the standard theory of cataclysmic variables, angular momentum loss (AML) via magnetic braking (MB) is stopped for fully convective stars. However, this period decrease is too large to be caused by AML via gravitational radiation (GR), indicating that there could be some extra source of AML beyond GR, but the predicted mass-loss rates from MB seem unrealistically large. The other possibility is that the O–C diagram may show a cyclic oscillation with a period of 7.72 years and a small amplitude of $0^{\rm d}.000525$. The cyclic change can be explained as the light-travel-time effect via the presence of a third body because the required energy for the magnetic activity cycle is much larger than that radiated from the secondary in a whole cycle. The mass of the potential third body is determined to be $M_3 \sin i' = 0.0189(\pm 0.0016)\, M_{\odot}$ when a total mass of 0.71 $M_{\odot}$ for SDSS J143547.87+373338.5 is adopted. For orbital inclinations $i' \geqslant 15\overset{\circ}{.}9$, it would be below the stable hydrogen-burning limit of $M_3 \sim 0.072\, M_{\odot}$, and thus the third body would be a brown dwarf.

Key words: binaries: close – binaries: eclipsing – brown dwarfs – stars: individual (SDSS J143547.87+373338.5) – stars: low-mass – white dwarfs

1. INTRODUCTION

Post-common envelope binaries (PCEBs) are usually detached binary systems that have orbital periods of a few hours to a week or so with a peak centered on ~8.1 h in a normal distribution in $\log(P_{\rm orb})$ (e.g., Nebot Gómez-Morán et al. 2011; Rebassa-Mansergas et al. 2012). Eclipsing PCEBs offer a unique opportunity to study the evolution of close binaries. Most of them contain a white dwarf primary and a red dwarf secondary where both components are well within their Roche lobes (e.g., Parsons et al. 2013). Although the white dwarf may accrete material from the secondary (e.g., Tappert et al. 2011), the accretion is very low through stellar wind. The detached configurations indicate that no mass transfer and accretion disks are present in these systems (those are observed in cataclysmic variables (CVs)), and hence the eclipses are not distorted by these effects. Moreover, because of the small size and compact structure of the white dwarf component, eclipse times of this type of binary system can be determined with a high precision and could be used to measure the orbital period and its rate of change by analyzing the observed–calculated (O–C) curve. This measurement provides valuable information on the evolution of CVs (e.g., Qian et al. 2015). On the other hand, they are also very good sources that can be used to search for and to investigate circumbinary substellar objects by analyzing the light-travel-time effect. If there is a substellar companion to the white dwarf eclipsing binary, the wobble of the binary's barycenter will cause the mid-eclipse arrival time to show a cyclic change, and brown dwarfs and planets hosted in those binaries can be detected. To search for substellar objects orbiting white dwarf binaries, we started to monitor selected eclipsing white dwarf binaries photometrically since 2009 (e.g., Qian et al. 2009, 2010b, 2012).

SDSS J143547.87+373338.5 (hereafter J1435) is a detached eclipsing binary with a white dwarf as the primary component (e.g., Eisenstein et al. 2006). Measurements by Rebassa-Mansergas et al. (2007) gave a mass range of 0.35–0.58 $M_{\odot}$ for the WD component. The eclipsing nature was discovered by Steinfadt et al. (2008) and the transit time is about 480 s. The WD in J1435 undergoes partial eclipses by an M-type companion every 3.015 hr. The spectral type of the low-mass secondary is M4-M6, which is a fully convective star, and contributes less than 4% to the total brightness in the blue-band BG-39 filter (e.g., Steinfadt et al. 2008). Time-resolved spectroscopic observations were later published by Pyrzas et al. (2009) and parameters of the system were revised. It was shown that the primary is a He-core white dwarf.

By using three eclipse times, the orbital period of J1435 was first determined by Steinfadt et al. (2008) as 0.12562974(55) d. The orbital period of the binary was later revised by Pyrzas

[7] Visiting Astronomer, Complejo Astronómico El Leoncito operated under agreement between the Consejo Nacional de Investigaciones Científicas y Técnicas de la República Argentina and the National Universities of La Plata, Córdoba and San Juan.

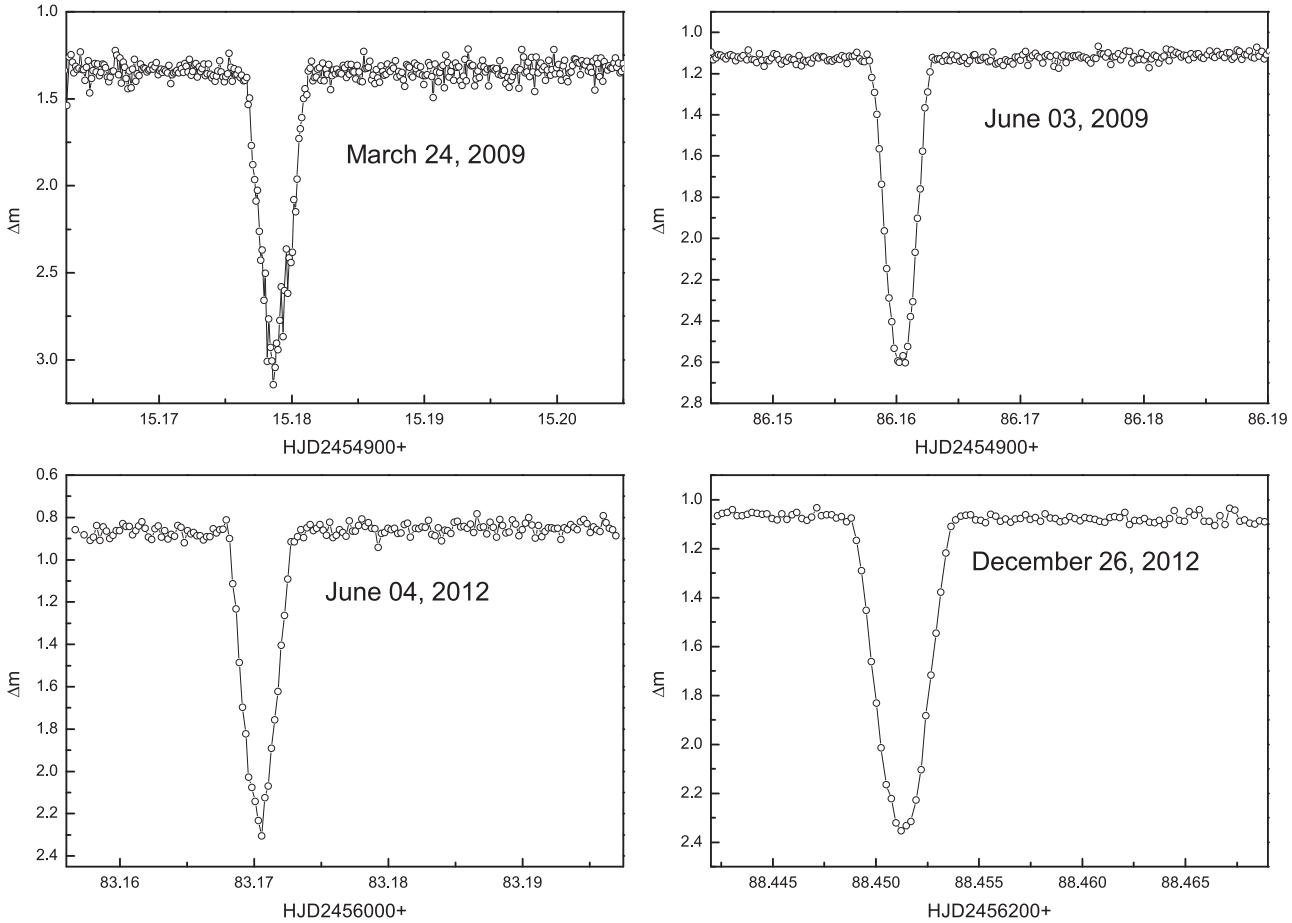

Figure 1. Several eclipse profiles of J1435 observed by using the 2.4-m telescope in the Lijiang observational station of Yunnan observatories.

et al. (2009) as 0.1256311(1) d by using their new determined eclipse times together with those published by Steinfadt et al. (2008). To understand the properties of the variations in the orbital period of J1435, it has been monitored since 2009 March 24, with the 2.4-m telescope in Lijiang observational station of Yunnan Observatories. Here we report the discovery of the rapid decrease in the orbital period of J1435 that reveals some extra source of angular momentum loss (AML) beyond gravitational radiation (GR) or/and the presence of a tertiary companion, most likely a brown dwarf companion to this binary system.

2. NEW CCD PHOTOMETRIC OBSERVATIONS FOR J1435

The eclipsing white dwarf binary, J1435, was monitored since 2009 March 24, by using the 2.4-m telescope in the Lijiang observational station of Yunnan observatories. During the observation in 2009, a VersArray 1300B CCD camera was attached to the 2.4-m telescope. The read-out time of the CCD camera is 1.8 s and the integration time for each CCD image was 8 s. As for the observations in 2012, YFOSC (Yunnan Faint Object Spectrograph and Camera) mounted on the 2.4-m telescope was used, which has a $2\,\mathrm{K} \times 4\,\mathrm{K}$ camera and its read-out time is about 2.95 s. Four eclipse profiles observed with the Lijiang 2.4-m telescope in 2009 and 2012 are displayed in Figure 1. The R-band filter was used during the observation on 2009 March 24. However, as we can see in the figure, the data show a large scatter. To improve the precision of the photometric data, no filters were used for later observations. With our observations, five mid-eclipse times were obtained and are listed in Table 1.

Table 1
New CCD Mid-eclipse Times for J1435

J.D. (Hel.) +2400000 (days)	Errors days	Filters	Telescopes
2454915.17879	0.00003	R	Lijiang 2.4-m
2454978.11992	0.00005	N	Lijiang 2.4-m
2454986.16034	0.00001	N	Lijiang 2.4-m
2456083.17039	0.00002	N	Lijiang 2.4-m
2456288.45127	0.00001	N	Lijiang 2.4-m
2456658.43424	0.00001	N	Thai 2.4-m
2457094.37349	0.00001	N	Thai 2.4-m
2457123.39425	0.00002	N	Thai 2.4-m

To obtain more data, the binary star was monitored by using the 2.4-m Thai National Telescope (TNT) of National Astronomical Research Institute of Thailand (NARIT) since 2013 December 31. This telescope is located on one of the highest ridges of Doi Inthanon (about 2457-m above sea level), the tallest peak in Thailand. The observing conditions (seeing and photometric conditions) of this site are very good during the dry season that runs approximately from November to April. The TNT is a Ritchey–Chrètien with two Nasmyth focuses. The ULTRASPEC fast camera mounted on the telescope was used for the observation on 2013 December

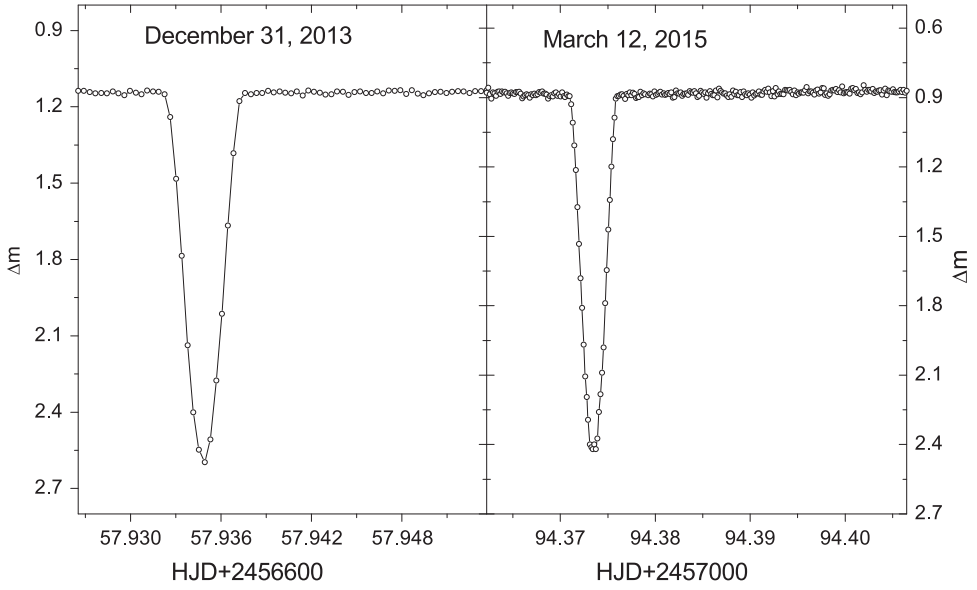

Figure 2. Two eclipse profiles of J1435 obtained with the 2.4-m telescope of NARIT. They were obtained on 2013 December 31 and 2015 March 12, respectively.

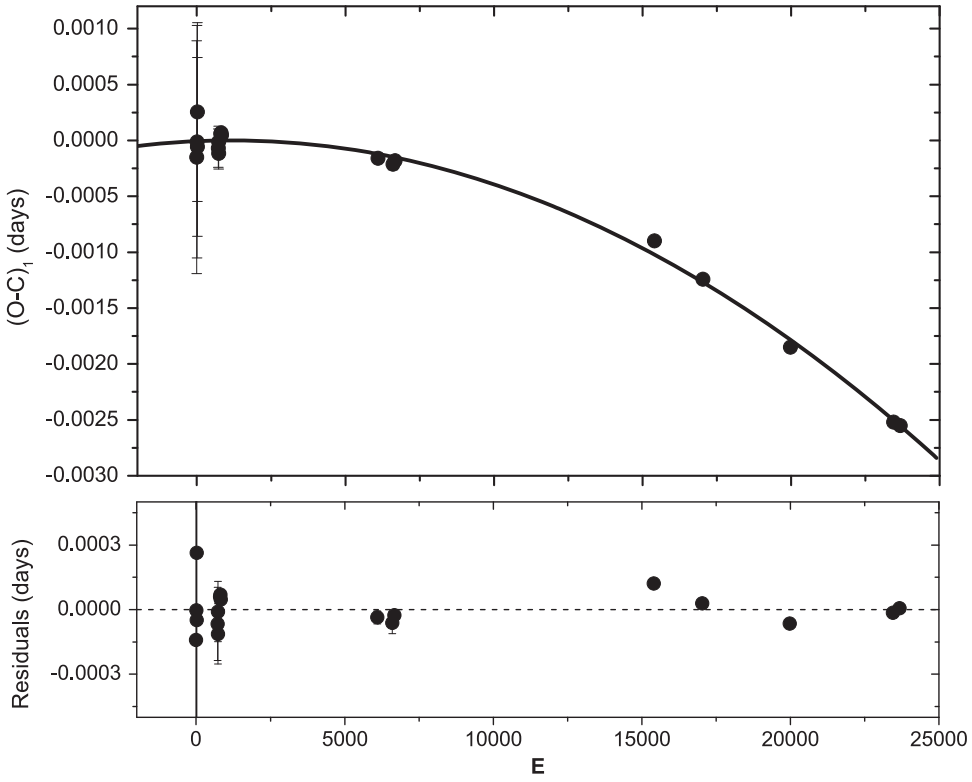

Figure 3. Plot of the $(O–C)_1$ diagram of J1435 with respect to the linear ephemeris given by Pyrzas et al. (2009) is shown in the upper panel. The solid line in the panel indicates a downward parabolic change revealing a continuous decrease at a rate of $\dot{P} = -2.94 \times 10^{-8}$ days year^{-1}. After the period decrease is removed, the residuals are shown in the lower panel.

31. It is the ULTRASPEC low-noise, frame-transfer EMCCD camera. As for the observation on 2015 March 12, a 4K CCD photometer with a BVRI filter system was applied. The camera is a cryogenically cooled (liquid nitrogen, −110 C) dewar holding a E2V232-84 thinned, astronomy broadband AR coated, grade one CCD. Two of the eclipse profiles obtained by this telescope are shown in Figure 2 and the corresponding eclipse times are displayed in Table 1. As done by Steinfadt et al. (2008), those eclipse times were computed with the Kwee & van Woerden (1956) method. The eclipse profiles shown in Figures 1 and 2 are symmetric, indicating that they could be determined in high precision.

3. THE ORBITAL PERIOD CHANGES OF J1435

By using the eclipse times listed in Table 1 together with those obtained by Steinfadt et al. (2008) and by Pyrzas et al. (2009), the $(O–C)_1$ values with respect to the linear ephemeris

derived by Pyrzas et al. (2009) were computed,

$$\mathrm{Min.I} = \mathrm{HJD}\ 2454148.70361 + 0.1256311 \times E. \quad (1)$$

The corresponding $(\mathrm{O–C})_1$ diagram is shown in the upper panel of Figure 3. As shown in the panel, the variation of the $(\mathrm{O–C})_1$ curve may show a downward parabolic change indicating a long-term continuous decrease in the orbital period. A least-squares solution leads to the following equation,

$$\begin{aligned}\mathrm{Min.I} = {} & 2454148.703602(\pm 0.000007) \\ & + 0^{\mathrm{d}}.1256311119(\pm 0.0000000003) \times E \\ & - 5.05(\pm 0.02) \times 10^{-12} \times E^2. \end{aligned} \quad (2)$$

The quadratic term in this equation reveals a continuous decrease at a rate of $\dot{P} = -2.94 \times 10^{-8}$ days year^{-1} (or -8.04×10^{-11} s s^{-1}).

J1435 is a short-period ($P \sim 3$ hr) close binary with a white dwarf primary and a red dwarf secondary. The continuous period decrease may be caused by AML due to GR. By using the following equation (e.g., Kraft et al. 1962; Faulkner 1971),

$$\frac{\dot{P}}{P} = -3\frac{32G^3}{5c^5}\frac{M_1M_2(M_1+M_2)}{d^4}, \quad (3)$$

the contribution of GR to the period decrease was computed to be $\dot{P}_{\mathrm{GR}} = -0.0081 \times 10^{-11}$ s s^{-1}. P in the equation is the orbital period, M_1 and M_2 are the masses of the primary and secondary, d is the distance between both components, G is the gravitational constant, and c is the speed of light. The derived value is about three orders smaller than the observed one ($\dot{P} = -8.04 \times 10^{-11}$ s s^{-1}). Therefore, the observed continuous decrease in the orbital period could not be explained by AML via GR.

The other mechanism that could cause the decrease in the orbital period is AML via magnetic braking (MB) of the secondary component. According to the standard theory of CVs, MB ceases when the secondary star becomes fully convective (e.g., Skumanich 1972; Verbunt & Zwaan 1981; Rappaport et al. 1983; Schreiber et al. 2010). However, some investigations showed that MB may not be completely stopped for fully convective stars (e.g., King et al. 2002; Pretorius & Knigge 2008; Qian et al. 2015). The secondary component in J1435 is a fully convective star. The rapid decreasing in the orbital period may be evidence of AML due to MB of the fully convective component.

We also consider the other possibility that the O–C curve may show a cyclic variation with a long period. By using the least-squares method, we determined

$$\begin{aligned}\mathrm{Min.I} = {} & 2454148.704123(\pm 0.000039) \\ & + 0^{\mathrm{d}}.125630992(\pm 0.000000003) \times E \\ & + 0.000525(\pm 0.000043)\sin[0^{\circ}.01604 \\ & \times (\pm 0.00010) \times E + 257^{\circ}.9(\pm 4^{\circ}.5)]. \end{aligned} \quad (4)$$

The linear ephemeris refers to the revisions of the initial epoch and the orbital period (dashed line in the upper panel of Figure 4). The cyclic oscillation has an amplitude of 45.4 s and a period of 7.72 years. The $(\mathrm{O–C})_2$ values calculated with the linear ephemeris in the equation are plotted in the middle panel of Figure 4 where the cyclic change is seen more clearly. After the revision of the orbital period and the cyclic change were subtracted from the $(\mathrm{O–C})_1$ curve, the residuals are displayed in the lowest panel.

4. DISCUSSIONS AND CONCLUSIONS

As discussed in the previous section, GR is insufficient to cause the observed period decrease. Additional AML via MB is required to explain the rate of period decrease. By using the following equation (Tout & Hall 1991),

$$\frac{\dot{P}}{P} = -2\left(\frac{R_{\mathrm{A}}}{d}\right)^2\frac{M}{M_1M_2}\dot{m}, \quad (5)$$

a computation yields $R_{\mathrm{A}}{}^2\dot{m} = 1.54 \times 10^{-8}$ in units of $R_{\odot}{}^2M_{\odot}$ yr^{-1}. R_{A} in Equation (5) is the Alfvén radius. The relation between the mass-loss rate ($\dot{m}$) and the Alfvén radius (R_{A}) is shown in Figure 5. If the Alfvén radius equals that of the Sun (i.e., $R_{\mathrm{A}} = 15R_{\odot}$), the required mass-loss rate is $\dot{m} = -6.82 \times 10^{-11}M_{\odot}$ per year. When $R_{\mathrm{A}} = 15R_2 = 3.45\,R_{\odot}$, the mass-loss rate is determined to be $\dot{m} = -1.29 \times 10^{-9}M_{\odot}$ yr^{-1}. Since the Alfvén radius is unknown, we could not determine the mass-loss rate for a fully convective star. The period decrease may be the evidence for the conclusion that magnetic braking does not cease for the fully convective component. However, the required mass-loss rates from MB seem unrealistically large. In the most extreme case, the mass-loss rate is $\dot{m} \sim 10^{-9}M_{\odot}$ yr^{-1}, which would imply that the entire M star would evaporate in a gigayear! The rate of $\dot{m} \sim 10^{-11}M_{\odot}$ yr^{-1} is also extreme, approaching CV levels of mass loss. Therefore, additional orbital AML may be caused by a circumbinary disk (e.g., Spruit & Taam 2001; Taam & Spruit 2001). The circumbinary disk was thought to be effective in draining orbital angular momentum from the system, which is one of the possible mechanisms driving the evolution of CVs.

The other possibility is that the O–C diagram may show a cyclic variation with a period of 7.72 years. The cyclic changes of the O–C diagram for close binaries containing at least one cool component could be explained by the solar-type magnetic activity cycles, i.e., the Applegate mechanism (Applegate 1992). In the mechanism, a certain amount of angular momentum is assumed to be periodically exchanged between the inner and the outer parts of the convection zone, and therefore the rotational oblateness and thus the orbital period will vary when the cool component goes through its activity cycles. The secondary in J1435 is a fully convective star that rotates mainly as a rigid body and lacks the thin interface layer between a radiative core and a convective envelope, where dynamo processes are thought to concentrate for solar-type stars (e.g., Barnes et al. 2005). To check whether or not this mechanism could explain the cyclic variation, the required energies to produce the cyclic oscillation for different shell masses of the secondary have been calculated with the same method used by Brinkworth et al. (2006) in the case of the pre-CV NN Ser. It is found that the required energies are larger than the total radiant energy of the M4.5-type component star in one whole cyclic change (see Figure 6). During the calculation, the parameters given by Pyrzas et al. (2009) were used, i.e., $M_1 = 0.50\,M_{\odot}$, $M_2 = 0.21\,M_{\odot}$, and $R_2 = 0.23\,R_{\odot}$. By using Kepler's third law,

$$(M_1 + M_2) = 0.0134a^3/P^2, \quad (6)$$

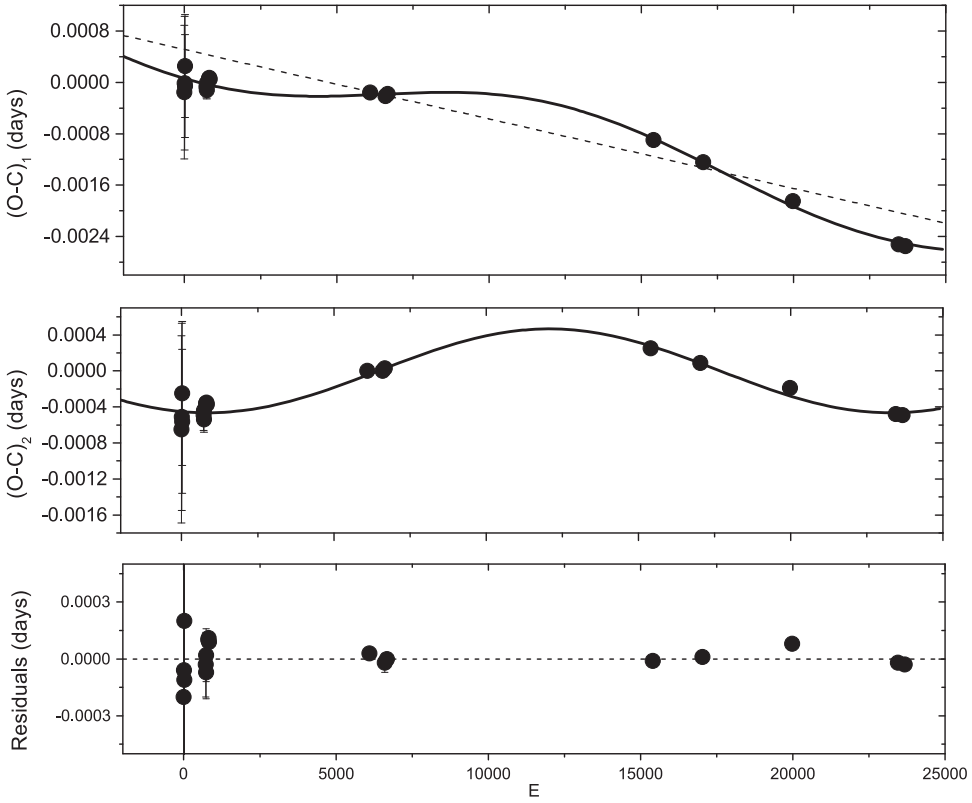

Figure 4. Solid line in the upper panel suggests a combination of a cyclic change and a revision in the orbital period, while the dashed line refers to the revised linear ephemeris. The theoretical light-travel time effect orbit of the potential brown dwarf companion with respect to the new ephemeris in Equation (4) is shown in the middle panel where the cyclic variation can be seen more clearly. All of the variations were removed, and the residuals are shown in the lower panel.

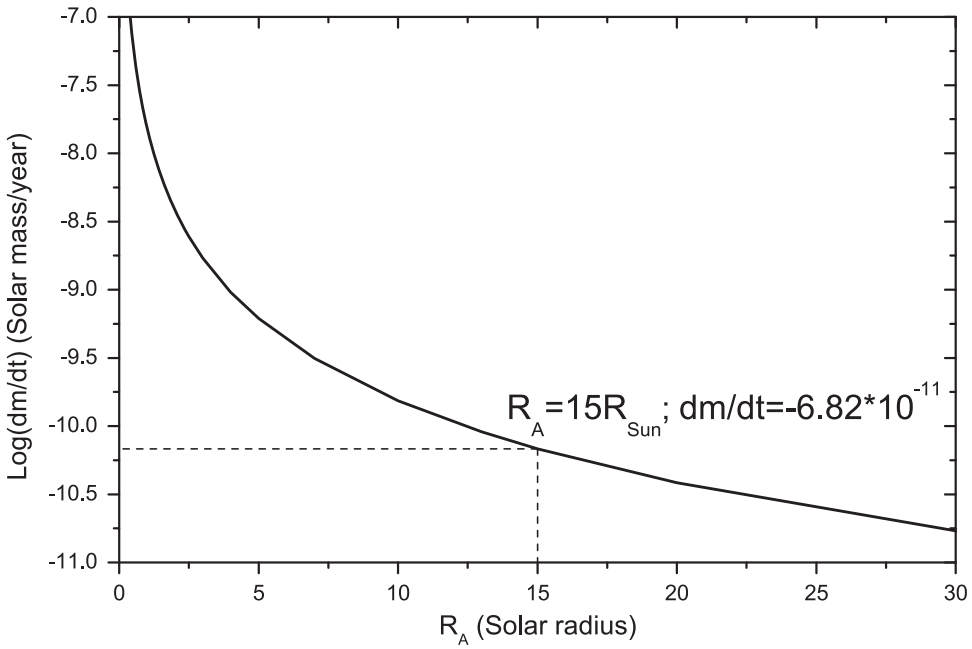

Figure 5. Relation between the mass-loss rate and the Alfvén radius in order to produce the continuous period decrease due to MB. When the Alfvén radius equals that of the Sun ($R_A = 15R_\odot$), the derived mass-loss rate in the magnetic stellar wind is $\dot{m} = -6.82 \times 10^{-11} M_\odot$ per year.

the orbital separation of the two component stars was computed as $a = 0.94\ R_\odot$. We choose a temperature of $T_2 = 3200$ K for the M4.5-type star and its luminosity was calculated by using $L_2 = \left(\frac{R_2}{R_\odot}\right)^2 \left(\frac{T_2}{T_\odot}\right)^4 L_\odot$. The result suggests that the mechanism of Applegate has difficulty interpreting the cyclic variation, though the basic quadrupole deformation idea cannot be so easily dismissed (e.g., Lanza 2006).

Therefore, we analyzed the O–C diagram of J1435 for the light-time effect that arises from the gravitational influence of a

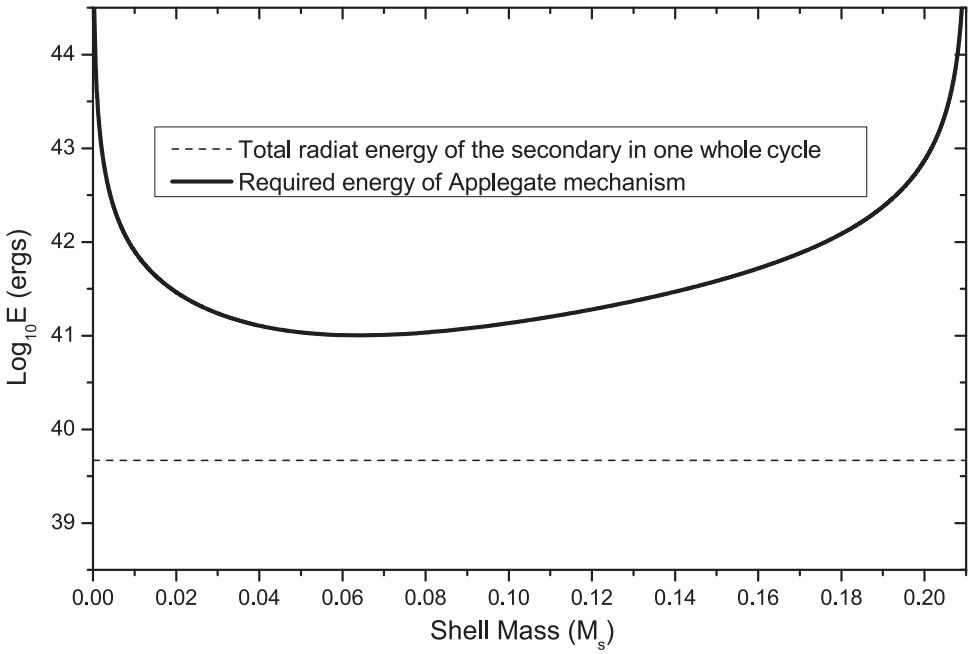

Figure 6. Plot of the energy required to cause the period oscillation of J1435 by using Applegate's mechanism as a function of the assumed shell mass of the cool component (solid line). The dashed line represents the total radiant energy of the secondary component star in a whole cyclic change of the O–C variation.

potential third body. The timespan of the data is about 8.14 years, which is close to the determined period (7.72 years) of the O–C oscillation. This indicates that the data cover is insufficient to determine the eccentricity of the third body. By simply assuming that the orbit of the third body is circular, its orbital and physical parameters were estimated. The projected orbital radius of J1435 rotating around the barycenter of the triple system is computed with the equation,

$$d'_{12} \sin i' = K \times c, \tag{7}$$

where K is the amplitude of the cyclic variation and c is the speed of light. Then, by using the absolute parameters determined by Pyrzas et al. (2009), a calculation with the following equation,

$$f(m) = \frac{4\pi^2}{GP_3^2} \times (d'_{12} \sin i')^3 = \frac{(M_3 \sin i')^3}{(M_1 + M_2 + M_3)^2}, \tag{8}$$

yields the mass function and the mass of the tertiary companion as: $f(m) = 1.26(\pm 0.31) \times 10^{-5}\, M_\odot$ and $M_3 \sin i' = 0.0189(\pm 0.0016)\, M_\odot = 19.8(\pm 1.7)\ M_{\rm Jup}$, respectively. G and P_3 in this equation are the gravitational constant and the period of the $(O–C)_2$ oscillation. If the orbital inclination of the tertiary companion is larger than 15°.9, the mass of the third body corresponds to $M_3 \leqslant 0.072\, M_\odot$, and thus it should be a brown dwarf. Therefore, with 82.3% probability, the third body is a brown dwarf (by assuming a random distribution of orbital plane inclination). The orbital radius d_3 of the tertiary component is about 3.42 AU when the orbital inclination equals 90° indicating that the orbit is very tight (3.42 AU). Assuming a $\sim 2\ M_\odot$ progenitor for the white dwarf, we may think that adiabatic mass loss would have put this object originally at an orbit of ~1.1 AU, which is comparable to the original separation of the binary, i.e., completely unstable. However, during this estimation, we ignore tidal interaction for lack of knowledge. The tidal interaction could lead to an enhance mass loss before the common envelope (CE) phase that might increase the survivability of planets and brown dwarfs during the CE (e.g., Bear & Soker 2010). Moreover, the circumbinary companion may be of the second generation, as discussed below.

Substellar objects orbiting white dwarfs are rare. To date only a few brown dwarf companions of white dwarfs were found (e.g., Becklin & Zuckerman 1988; Farihi & Christopher 2004; Dobbie et al. 2005; Burleigh et al. 2006; Maxted et al. 2006). As for white dwarf binary stars, a few exoplanets or brown dwarfs were reported to be orbiting V471 Tau (Guinan & Ribas 2001), QS Vir (Qian et al. 2010b; Almeida & Jablonski 2011), NN Ser (Marsh et al. 2014), and RR Cae (Qian et al. 2012). The presence of a brown dwarf candidate to the white dwarf-red dwarf binary J1435 will provide us with more knowledge regarding the formation and evolution of substellar objects. On the other hand, some of those circumbinary objects were ruled out by considering dynamical instabilities (e.g., Horner et al. 2012, 2013; Wittenmyer et al. 2013; Bours et al. 2014). However, more precision data and detailed investigations are required to confirm them in the future. Moreover, it should be noted that the proposed brown dwarf around V471 Tau was ruled out by Hardy et al. (2015), while a new investigation favors a brown dwarf companion about 12 AU from the eclipsing binary (Vaccaro et al. 2015).

J1435 is a pre-CV system with an orbital period of three hours that is just at the upper edge of the period gap of CVs. It is formed through a CE evolution and will evolve into normal CVs by secular AML via GR and MB (e.g., Shimansky et al. 2006). The brown dwarf orbiting J1435 may suggest that some short-period CVs should contain substellar companions. A possible planet was found to be orbiting the eclipsing dwarf nova V893 Sco and V2051 Oph (e.g., Bruch 2014; Qian et al. 2015). A few planetary candidates orbiting the two magnetic CVs, DP Leo (Qian et al. 2010a; Beuermann et al.

2011) and HU Aqr (Qian et al. 2011; Goździewski et al. 2015), were reported. To check this conclusion, photometric monitoring of some deeply eclipsing CVs (e.g., V2051 Oph) is required.

One interesting question arises here: why do virtually all of the white dwarf plus main-sequence star binaries with good timing coverage show O–C variations? If these changes are caused by the presence of circumbinary companions, why are they so common? On the other hand, substellar objects orbiting single white dwarfs are so rare. This may be caused by the fact that the evolutions of binaries are quite different from those of single stars. These binary stars have undergone the CE evolution. The low-mass stars in the original binaries spiraled in the CE after the more massive stars evolved into a red giant or an AGB star. The ejection of the CE removed a large amount of angular momentum, and then the short-period close binaries were formed. It is possible that the spiraling process of the low-mass stars in CE protected those circumbinary objects. The other possibility is that they are second generation exoplanets or brown dwarfs formed during the late evolution of binary stars (e.g., Vöschow et al. 2014).

This work is partly supported by the Chinese Natural Science Foundation (No. 11133007 and No. 11325315), the Key Research Program of the Chinese Academy of Sciences (Grant No. KGZD-EW-603), the Science Foundation of Yunnan Province (Nos. 2012HC011 and 2013FB084), and by the Strategic Priority Research Program "The Emergence of Cosmological Structures" of the Chinese Academy of Sciences (No. XDB09010202). New CCD photometric observations of SDSS J143547.87+373338.5 were obtained with the 2.4-m Thai National Telescope (TNT) of National Astronomical Research Institute of Thailand and with the 2.4-m telescopes in Lijiang station of Yunnan Observatories.

REFERENCES

Almeida, L. A., & Jablonski, F. 2011, IAUS, 276, 495
Applegate, J. H. 1992, ApJ, 385, 621
Barnes, J. R., Cameron, A. C., Donati, J.-F., et al. 2005, MNRAS, 357, L1
Bear, E., & Soker, N. 2010, NewA, 15, 483
Becklin, E. F., & Zuckerman, B. 1988, Natur, 336, 656
Beuermann, K., Buhlmann, J., Diese, J., et al. 2011, A&A, 526, A53
Bours, M. C. P., Marsh, T. R., Breedt, E., et al. 2014, MNRAS, 445, 1924
Brinkworth, C. S., Marsh, T. P., Dhillon, V. S., & Knigge, C. 2006, MNRAS, 365, 287
Bruch, A. 2014, A&A, 566, A101
Burleigh, M. R., Hogan, E., Dobbie, P. D., et al. 2006, MNRAS, 373, L55
Dobbie, P. D., Burleigh, M. R., Levan, A. J., et al. 2005, MNRAS, 357, 1049
Eisenstein, D. J., Liebert, J., Harris, H. C., et al. 2006, ApJS, 167, 40
Farihi, J., & Christopher, M. 2004, AJ, 128, 1868
Faulkner, J. 1971, ApJ, 170, 99
Goździewski, K., Slowikowska, A., Dimitrov, D., et al. 2015, MNRAS, 448, 1118
Guinan, E. F., & Ribas, I. 2001, ApJL, 546, L43
Hardy, A., Schreiber, M. R., Parsons, S. G., et al. 2015, ApJL, 800, L24
Horner, J., Hinse, T. C., Wittenmyer, R. A., Marshall, J. P., & Tinney, C. G. 2012, MNRAS, 427, 2812
Horner, J., Wittenmyer, R. A., Hinse, T. C., et al. 2013, MNRAS, 435, 2033
King, A. R., Schenker, K., & Hameury, J. M. B. 2002, MNRAS, 335, 513
Kraft, R. P., Matthews, J., & Greenstein, J. L. 1962, ApJ, 136, 312
Kwee, K. K., & van Woerden, H. 1954, BAN, 12, 327
Lanza, A. F. 2006, MNRAS, 369, 1773
Marsh, T. R., Parsons, S. G., Bours, M. C. P., et al. 2014, MNRAS, 437, 475
Maxted, P. F. L., Napiwotzki, R., Dobbie, P. D., et al. 2006, Natur, 442, 543
Nebot Gómez-Morán, A., Gänsicke, B. T., Schreiber, M. R., et al. 2011, A&A, 536, A43
Parsons, S. G., Gänsicke, B. T., Marsh, T. R., et al. 2013, MNRAS, 429, 256
Pretorius, M. L., & Knigge, C. 2008, MNRAS, 38, 1485
Pyrzas, S., Gänsicke, B. T., Marsh, T. R., et al. 2009, MNRAS, 394, 978
Qian, S.-B., Dai, Z.-B., Liao, W.-P., et al. 2009, ApJL, 706, L96
Qian, S.-B., Han, Z.-T., Fernández Lajús, E., et al. 2015, ApJS, 221, 17
Qian, S.-B., Liao, W.-P., Zhu, L.-Y., & Dai, Z.-B. 2010a, ApJL, 708, L66
Qian, S.-B., Liao, W.-P., Zhu, L.-Y., et al. 2010b, MNRAS, 401, L34
Qian, S.-B., Liu, L., Liao, W.-P., et al. 2011, MNRAS, 414, L16
Qian, S.-B., Liu, L., Zhu, L.-Y., et al. 2012, MNRAS, 422, L24
Rappaport, S., Joss, P. C., & Verbunt, F. 1983, ApJ, 275, 713
Rebassa-Mansergas, A., Gänsicke, B. T., Rodríguez-Gil, P., Schreiber, M. R., & Koester, D. 2007, MNRAS, 382, 1377
Rebassa-Mansergas, A., Zorotovic, M., Schreiber, M. R., et al. 2012, MNRAS, 423, 320
Schreiber, M. R., Gänsicke, B. T., Rebassa-Mansergas, A., et al. 2010, A&A, 513, L7
Shimansky, V., Sakhibullin, N. A., Bikmaev, I., et al. 2006, A&A, 456, 1069
Skumanich, A. 1972, ApJ, 171, 565
Spruit, H. C., & Taam, R. E. 2001, ApJ, 548, 900
Steinfadt, J. D. R., Bildsten, L., & Howell, S. B. 2008, ApJL, 677, L113
Taam, R. E., & Spruit, H. C. 2001, ApJ, 561, 329
Tappert, C., Gänsicke, B. T., Schmidtobreick, L., & Ribeiro, T. 2011, A&A, 532, A129
Tout, C. A., & Hall, D. S. 1991, MNRAS, 253, 9
Vaccaro, T. R., Wilson, R. E., Van Hamme, W., & Terrell, D. 2015, ApJ, 810, 157
Verbunt, F., & Zwaan, C. 1981, A&A, 100, L7
Vöschow, M., Banerjee, R., & Hessman, F. V. 2014, A&A, 562, A19
Wittenmyer, Robert, A., Horner, J., & Marshall, J. P. 2013, MNRAS, 431, 2150